Packing Structures and Packing Effects on Excitation Energies of Amorphous Phase Oligothiophenes

Guiling Zhang,[†,‡] Yong Pei,[†] and Jing Ma*[,†]

Department of Chemistry, Institute of Theoretical and Computational Chemistry, Lab of Mesoscopic Materials Science, Nanjing University, Nanjing, 210093, P. R. China, and Department of Chemistry, Harbin Normal University, Harbin, 150080, P. R. China

Kailiang Yin

Department of Chemical Engineering, Jiangsu Polytechnic University, Changzhou, 213016, P. R. China

Cheng-Lung Chen

Department of Chemistry, National Sun Yat-Sen University, Kaohsiung, Taiwan, 80424, P. R. China

Received: December 16, 2003; In Final Form: March 8, 2004

The packing structures and packing effects on excitation energies of thiophene, terthiophene, sexithiophene, and duodecithiophene are studied by employing the molecular dynamic (MD) simulations and the TDDFT/6-311++G** calculations. It has been demonstrated by MD simulations that (1) when going from short to long chain systems, the packing structure prefers to be in the π-stacked form and (2) the effective conjugation lengths, ECLs, of terthiophene, sexithiophene, and duodecithiophene chains are 2, 3, and 4, respectively. Accordingly, the comprehensive effects of the interchain distance, *R*, and ECL on excitation energy can be estimated by a simple formula. The calculated excitation energies of the packing oligothiophenes are in agreement with the experimental data with the average deviation of 0.12 eV.

1. Introduction

Thiophene oligomers and polymers have received extensive experimental and theoretical attention because of their fascinating electronic and optical properties.[1,2] Electronic structures and spectra of the isolated oligothiophenes have been extensively studied by quantum chemical methods at various levels.[3−10] Those theoretical results have been employed to qualitatively and even quantitatively rationalize experimental observations with the common belief that in most cases the main electronic properties are governed by what appears in a single chain. For example, the Hückel model[11] and the valence effective Hamiltonian technique[3] were used to explain and predict the chain-length dependence of electronic properties of conjugated systems. On the other hand, many experiments[12,13] have guided theoretical interests to surveys of the role played by interchain interactions.[2,3,14] Theoretical efforts have been devoted to the following two main aspects of interchain interactions of thiophene oligomers: One active field is the exploration of the origin of intermolecular interactions of thiophene dimers by electron correlation methods such as many body perturbation theory (MBPT) and configuration interaction (CI) methods.[15] Another important direction is to understand the influence of the interchain interaction on optical properties, which has been elaborately addressed by pioneer works of Brédas and coworkers.[14,16−18] Despite the above-mentioned fruitful achievements in the understanding of intermolecular interactions in oligothiophene systems, there are two interesting questions stimulating us to carry out further investigations on the packing effects on properties of thiophene oligomers. (1) Most experimental and theoretical studies on packing structures are mainly focused on crystal structures. How about the packings of oligothiophenes in the amorphous phase and what is the trend in their packing configurations as the chain grows? (2) What is the comprehensive effect of the chain packings and torsions on excitation energies of oligothiophenes? However, investigations of packing structures for long-chain systems are beyond the capabilities of quantum chemistry (QM) methods. Molecular dynamics (MD) simulation is a universal tool used to detect the dynamic information of complicated systems, which will give a global packing picture of oligothiophenes. In this paper, we aim to answer the above two questions by combining MD simulations and time-dependent density functional theory (TDDFT) calculations.

Oligothiophenes (thiophene (**T**), terthiophene (**3T**), sexithiophene (**6T**), and duodecithiophene (**12T**)) are selected in our present theoretical studies not only because of their relatively higher stability than other π-conjugated oligomers[1,2,9] but also because of the abundant literature from both experimental and theoretical studies. The X-ray crystal structures of terthiophene and sexithiophene reveal that neighboring thiophene moieties are placed antiparallelly and take a "herringbone-type" (T-shaped) configuration with an angle between mean planes of adjacent molecules spanning from 55° to 70°.[19−23] The thiophene molecules in crystals are almost planar; the torsion angles between neighboring thiophene rings are about 6−9° in terthiophene[19] and 2° in sexithiophene.[22] But there are no unambiguous pictures of amorphous phase oligothiophenes and some evidence from solvatochromism and thermochromism shows that oligothiophene configurations are affected and

[†] Nanjing University.
[‡] Harbin Normal University.

10.1021/jp037882j CCC: $27.50
Published on Web 05/06/2004

SCHEME 1

Packing and torsion effects

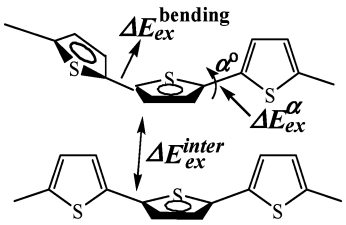

modified by the environment.[24] Therefore, we investigate the amorphous phase (rather than the crystal phase) to detect the intrinsic properties of oligothiophenes in their natural states.

The magnitude of excitation energy, E_{ex}, determines the intrinsic electronic and optical properties of the conjugated material.[10,14] It is well-known that both the planar distortions and the interchain distances affect the E_{ex} of the oligothiophene systems to some extent (cf. Scheme 1). Considering experimental measurements correspond to the statistically averaged values over various distributions, it is natural for us to correlate the statistic configurations obtained from MD simulations with the excitation energies of packing systems. Therefore, in the present work we employ MD simulations and TDDFT calculations to (1) investigate the changing tendency in packing structures from short to long chains of amorphous phase oligothiophene systems and (2) estimate the comprehensive effect of packing and torsions on the excitation energies of oligothiophene systems.

2. Computational Details

2.1. Validations of the Force Field. Packing structures of oligothiophene chains are reflected from inter-ring distances, π-stacked or T-shaped packing styles, and chain torsions, which can be obtained from trajectories of MD simulations. Thus, the performance of the polymer consistent force field (PCFF),[25] which is used in our simulations, is validated from the following three aspects.

Geometries. The geometries of thiophene (**A)** and the thiophene dimer (**B)** obtained by MP2/6-31+G* and PCFF optimizations, as well as the experimental data,[1] are given in Figure 1. We can see from Figure 1 that PCFF geometries agree with the available experimental data and the MP2/6-31+G* results (shown in brackets). Encouragingly, for the thiophene dimer (model **B**), the PCFF provides a reasonable prediction of the inter-ring distance in comparison with the MP2 packing structure.

Relatively Stabilities. To assess the accuracy of PCFF in predictions of the relative stabilities between packing structures, models **C** (T-shaped) and **D** (π-stacked), two typical packing dimers,[15] are chosen to make the comparison of the calculated packing energies between the CCSD(T) (coupled-cluster singles and doubles (triples))[15] and the PCFF calculations. The estimated CCSD(T) packing energies at the basis set limit are −2.05 and −1.59 kcal/mol for **C** and **D**, respectively,[15] while the packing energies calculated by PCFF are −1.34 kcal/mol for **C** and −0.86 kcal/mol for **D**. Although the PCFF method underestimates the packing energies of each packing pair by around 0.7 kcal/mol, the difference in packing energies between **C** and **D** obtained by PCFF (−0.46 kcal/mol) coincides well with that by the estimated CCSD(T) (−0.48 kcal/mol). That is, the relative stability of **C** to **D** is correctly predicted by PCFF calculations compared with the estimated CCSD(T) results.

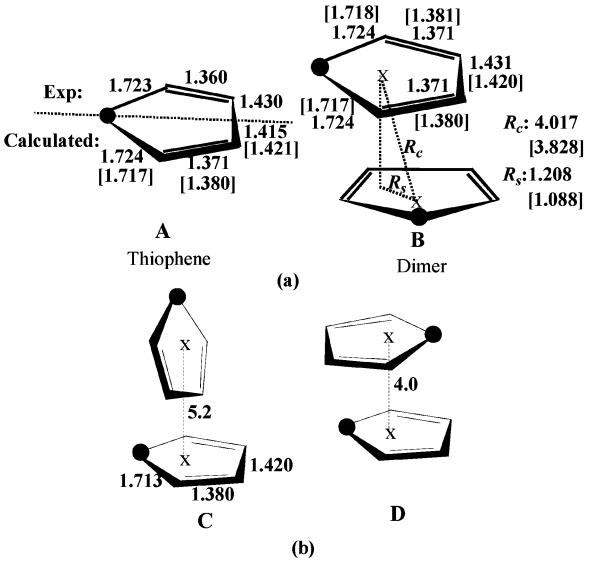

Figure 1. Models for validations of PCFF force field on (a) the optimized geometries and (b) the relative stability. The calculated values in part a are obtained from PCFF force field and MP2/6-31+G* (in the brackets) optimizations. The experimental data come from ref 1. The geometries of dimers in part b are taken from ref 15. All the listed data are in units of Å.

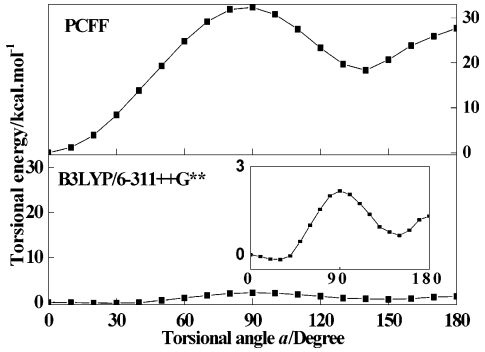

Figure 2. Validations of PCFF force field on torsional potentials of bithiophene. $\alpha = 0°$ means *trans*-bithiophene and $\alpha = 180°$ means *cis*-bithiophene.

Chain Torsions. We also perform calculations for the torsion potentials of bithiophene with the varied torsion angles α between 0° and 180° by the PCFF and B3LYP/6-311++G** methods, respectively. The resulting curves are plotted in Figure 2. It should be mentioned that there is a remarkable difference in values of torsional energy barriers between the B3LYP and PCFF calculations. The B3LYP computes the electronic energy, but the PCFF energy, also called steric energy, is the excess energy relative to a hypothetical molecule with noninteracting fragments and is strongly depended on the empirical force constants. So, we can only inspect the global shapes of torsion−potential curves. Both PCFF and B3LYP/6-311++G** calculations give peaks at the point of $\alpha = 90°$ (perpendicular conformation) and the local minima around $\alpha = 150°$ on curves (Figure 2). However, the B3LYP calculations yield another minimum at $\alpha = 30°$, which is absent in the PCFF torsion curve. The twisted structure with a torsion angle of about 30° predicted by the B3LYP calculations is slightly more stable than that of the trans structure ($\alpha = 0°$) by only 0.16 kcal/mol, in coincidence with the nonplanar conformation observed in the gas phase[26] and other calculations.[3,6] In fact, other force field methods, such as the universal force field (UFF) and consistent valence force field (CVFF), also lose the minimum at $\alpha = 30°$ with the results given in the Supporting Information. One should

be aware of the above-mentioned limitations of the present empirical force fields when a conclusion will be drawn from the torsion potentials obtained by force field methods. A further improvement of the empirical torsion potential used in current force fields is desired in our future works. On the other hand, our simulations on packing structures are conducted in the amorphous phase, which may be close to the solid state in which the bithiophene takes a planar trans conformation ($\alpha = 0°$).[27]

2.2. Molecular Dynamics Simulations. All MD simulations are performed in the NVT ensemble (constant number of particles, volume, and temperature). The temperature of the systems is set to 298 K by the Nosé-Hoover method. The PCFF is used in our calculations. The periodic boundary condition (PBC) is employed in all simulations. All MD simulations are performed on the SGI Origin200 workstation with Cerius^2 (Version 3.5) from Molecular Simulation Inc.[28]

Four kinds of oligothiophenes, **T**, **3T**, **6T**, and **12T**, are investigated in our simulations. The experimental density[1] of oligothiophenes is reported as 1.4 g/cm^3. At this density, the oligothiophene chains are packed so densely that variations of their configurations and orientations are difficult. To avoid being trapped into an insufficient distribution of orientations of oligothiophene chains, we start our MD simulations at a low density of 0.5 g/cm^3, in which oligothiophenes are loosely packed and there is enough space for chains to alter their relative orientations and configurations. The initial cell sizes for **T**, **3T**, **6T**, and **12T** systems are 17.75, 25.45, 32.03, and 40.32 Å, respectively, with 20 chains in each cell. MD simulations are carried out for 20 ps to equilibrate these systems and then the simulation boxes are reduced slightly (say, 0.3%) and another 20 ps of simulations are carried out to reach an equilibrium status. The above processes are repeated until the density arrives at the experimental value of 1.4 g/cm^3. Starting from these structures, the 200-ps MD simulations are subsequently carried out. Trajectories are collected at every 50-fs interval. Finally, we employ trajectories after 5 ps for the statistic analysis of packing structures of oligomer chains.

2.3. Time-Dependent Density Functional Theory (TD-DFT). TDDFT, a useful tool for predicting the excitation energies,[10,29−31] is employed to calculate the first dipole-allowed excitation energies of the thiophene chains. The B3LYP functional has been validated for many systems.[31−33] The TDDFT/B3LYP calculations are carried out at the level of 6-311++G** basis set as implemented in Gaussian 98[34] on the SGI 3800 workstation.

3. Results and Discussions

In this section, we first present the statistic distributions of packing configurations of oligothiophene systems with various chain lengths on the basis of MD simulation trajectories, and then we analyze the torsion and packing effects on excitation energies of the amorphous phase systems.

3.1. Packing Structures. The interchain distances, distributions of π-stacked vs T-shaped styles, and chain torsions are surveyed as follows to show the packing structures of oligomer chains.

Inter-ring Distances. The radial distribution functions, $f(r)$, of distances between two centers of mass of two thiophene rings in different chains are calculated by the following formula.

$$f(r) = n\langle\delta(r - R_c)\rangle \tag{1}$$

In eq 1, the bracket indicates the time average and R_c is the distance between two centers of mass of two rings in different chains; n is a normalization factor so that $\int_0^R f(r)\,dr = 1$, where R is the maximum distance between two rings in the simulation box. Plots of $f(r)$ for **T**, **3T**, **6T**, and **12T** are given in Figure 3. Evidently, there is a common turning point at about 6.5 Å for all four systems, implying that the effective interchain interaction region is within 6.5 Å. For the thiophene, **T**, the peak of $f(r)$ appears in the range of 4.5−5.5 Å; but for longer chains, **3T**, **6T**, and **12T**, the peaks shift to larger interchain separations of around 5.5 Å. When the inter-ring distances are below 4.0 Å, the populations are relatively small for four systems.

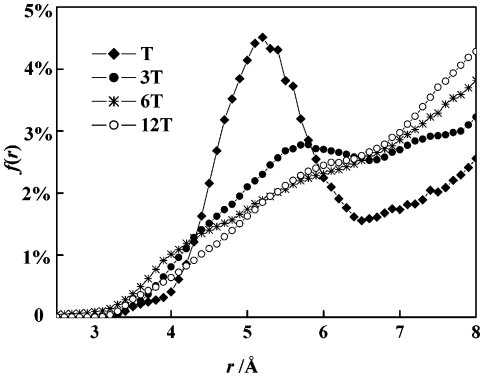

Figure 3. Radial distribution functions $f(r)$ of distances between two centers of mass of two thiophene rings in different chains of various packing systems.

π-Stacked vs T-Shaped Structures. Given in Figure 4 are the selected snapshots of **3T** and **12T** systems at 200 ps. The arrangement of chains in the **3T** system appears to be more disordered than that in the **12T** system. Usually the order parameters (S_{ij}) of thiophene rings are employed to describe the packing structures. Let vector $\vec{V}_i$ and $\vec{V}_j$ denote the unit normal vectors of the ith and jth thiophene rings (cf. Figure 5), respectively, then the order parameter between any pair of thiophene rings can be evaluated as

$$S_{ij} = \frac{3}{2}\langle\cos^2\theta_{ij}\rangle - \frac{1}{2} \tag{2}$$

where inclination of two rings, θ_{ij}, is the angle between $\vec{V}_i$ and $\vec{V}_j$, and the bracket refers to the time average. For two fully parallel rings, $\theta = 0°$, $S_{ij} = 1$, and for completely perpendicular pairs, $\theta = 90°$, $S_{ij} = -0.5$. Here we investigate the statistic distribution of angle θ.

We concentrate our survey on the effective inter-ring distances within 6.5 Å as already addressed in the above subsection. Population curves of packing configurations with variations of the inclination angles (θ) for **T**, **3T**, **6T**, and **12T** systems are depicted in Figure 5. A distinct feature can be clearly seen from Figure 5 that the peak of high population shifts from the T-shaped to π-stacked structure with the growth of chain lengths. In the system **T**, thiophene rings exist in mainly T-shaped packings with inclination of around 65° at 298 K. CCSD(T) calculations on the dimer models also suggest T-shaped conformations are slightly more stable than π-stacked ones at 0 K.[15] Both T-shaped and π-stacked packings appear in system **3T** with comparable populations, leading to a disorder alignment in the whole system as shown in the snapshot (Figure 4a). The π-stacked packing styles are more favorable than the T-shaped ones in the longer chain systems of **6T** and **12T**. In fact, the statistic π-stacked conformations are not strictly parallel packings but with small inclinations of about 15−40°. These inclinations in the amorphous phase are smaller than that of 55° in the crystal state of **6T** by X-ray investigation.[22] In the

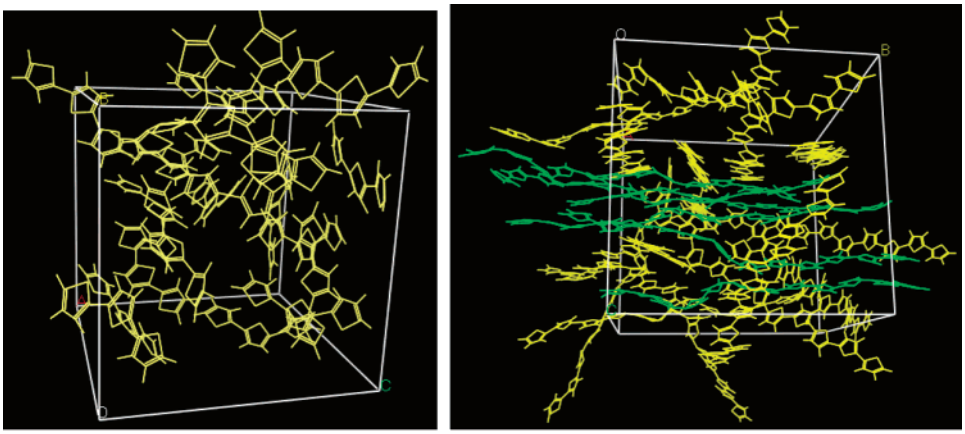

Figure 4. Snapshots of (a) terthiophene (**3T**) and (b) duodecithiophene (**12T**) systems from MD simulations at 200 ps. The green chains show they are strongly correlated in the **12T** system.

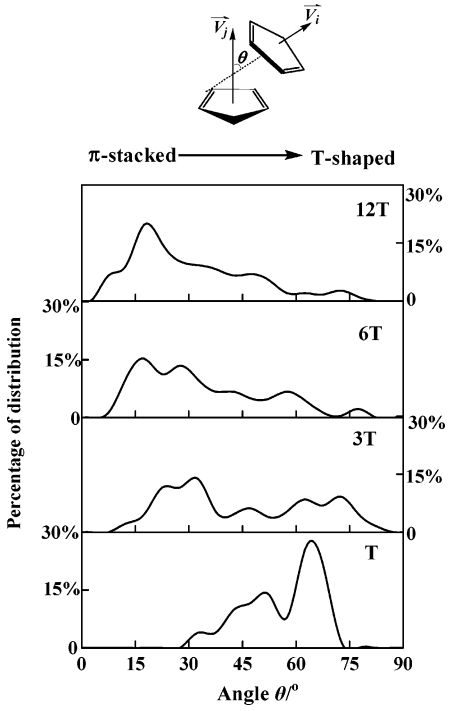

Figure 5. The distribution of packing pairs with the variation of inclination angle θ. For two fully parallel rings $\theta = 0°$ and for complete perpendicular pairs $\theta = 90°$.

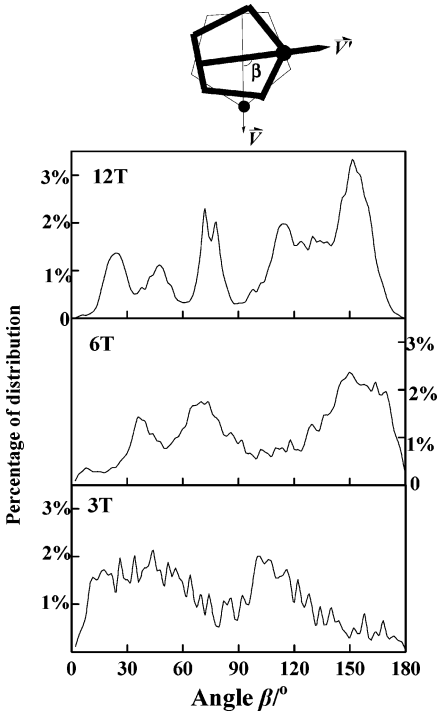

Figure 6. Distributions of configurations of π-stacked pairs for terthiophene (**3T**), sexithiophene (**6T**), and duodecithiophene (**12T**) systems with various rotational angle β.

dynamics of long-chain systems in the amorphous phase, thiophene chains present shapes of wavelike bending, which can be clearly seen from the snapshot of **12T** (Figure 4b). These fluctuations of the long chains are unfavorable in forming T-shaped packings.

The π-stacked packings with $\theta < 40°$ in oligothiophenes can be further characterized by the orientation angle β as defined in Figure 6. The populations of orientation angles (β) are drawn in Figure 6 to show the relative orientation of the π-stacked rings. For short chains in the **3T** system, the population of β spreads quite evenly from the cis to trans packings, showing a disorder packing behavior. The abundant distributions around $\beta = 150°$ manifest that longer chains are substantially trans correlated in **6T** and **12T** systems. Long-chain systems tend to be orderly arranged in trans π-stacked forms in the amorphous phase.

Chain Torsions. The bends of chains and rotations of inter-ring bonds are two major factors causing chain torsions away from planarity. The former is usually described by the head-to-tail distances of chains, and the latter by the inter-ring torsion angles α (as defined in Figure 2).

The statistically averaged distances between the terminal carbon atoms over the time evolution for **3T**, **6T**, and **12T** systems are 9.58, 20.05, and 40.18 Å, respectively. On average, chains in **3T**, **6T**, and **12T** are shortened by 0.24, 0.35, and 0.46 Å per thiophene unit, respectively, compared to their fully stretched forms. This indicates that the bending degree is enhanced when the chain becomes longer. The increasing flexibility with the chain elongation can be easily seen in Figure 4: the bends of **12T** chains lead to the shrinking of the head-to-tail distances.

Then, the torsion angles, α, are employed to describe the torsional distortion of chains. Figure 7a plots the distributions of α at every 5° interval. The torsion angles α are mostly distributed in the range of 5−10° for **3T**, **6T**, and **12T** systems. This is in agreement with the experimental observation that the

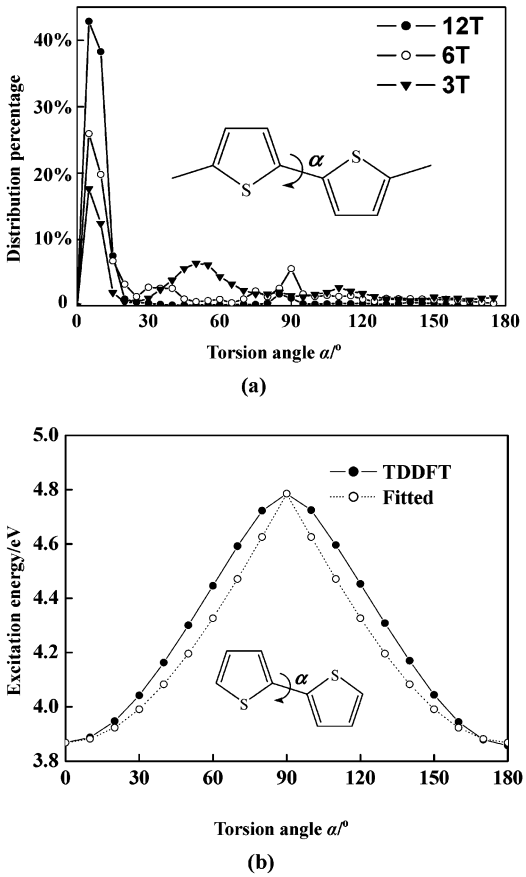

Figure 7. (a) The statistic distribution of inter-ring torsion angles α at an interval of 5° for terthiophene (**3T**), sexithiophene (**6T**), and duodecithiophene (**12T**) systems. (b) The dependence of excitation energies of bithiophene on the rotation angle α obtained from TDDFT calculations at the level of B3LYP/6-311++G** (solid line). The dotted line gives the fitted values according to a cosine function realized by Brédas and co-workers (cf. ref 4).

twist of two adjacent thiophene rings is about 6° to 9° for terthiophenes in the crystal phase.[19] Furthermore, in the amorphous phase of **3T**, another relatively high population (26%) in the range of $\alpha = 40-60°$ is also observed in our simulations, which indicates two major conformers coexist in the **3T** system. In experiments, the coexistence of two conformers is also observed for bithiophene partially oriented in the nematic phase of a liquid crystalline solvent[35] and in EPR measurements of the radical anion of bithiophene.[36] That is to say, the steric hindrance to rotate around the ring−ring linkage is small in short-chain systems. But for the longer chains, the inter-ring bond is not easy to rotate because of the strong steric hindrance coming from both sides of the inter-ring bond. So, in systems **6T** and **12T**, only one high peak, corresponding to a slightly twisted trans conformation, exists.

The chain torsions destroy the extent of the π-conjugation by which some physical and chemical properties are determined. It has been well-recognized that π-conjugated systems have relatively lower excitation energies due to the narrow gaps between the highest occupied and the lowest unoccupied orbitals. It can be anticipated that the excitation energy of the thiophene oligomer will be increased by chain torsions. To show the influence of chain torsions on the excitation energies in a more quantitative way, we perform TDDFT calculations using B3LYP functional at the 6-311++G** basis set on the bithiophene with different torsion angle α ranging from 0° to 180°. Figure 7b gives a monotonically increasing curve of excitation energies when two rings are transformed from the planar to perpendicular

SCHEME 2

Conjugation length (*CL*) and effective conjugation length (*ECL*)

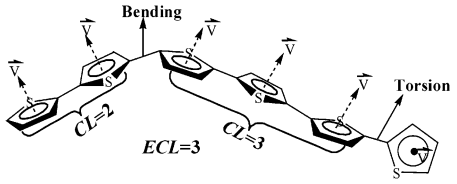

configurations. As suggested by Brédas and co-workers,[4] the TDDFT excitation energies also can be fitted with a cosine function, $E_\alpha = E_{\alpha=0} + [(E_{\alpha=90} - E_{\alpha=0})] \times (1 \pm \cos\alpha)]$. The fitted curve (dotted line in Figure 7b) agrees well with that from the TDDFT calculations.

In addition, since the slight nonplanarity (α is smaller than 10° or larger than 170°) does not cause obvious changes in the excitation energies (less than 0.02 eV) relative to that of the planar chain, we take the value of $S \geq 0.955$, corresponding to $\alpha \leq 10°$ or $\alpha \geq 170°$, to judge the planarity of a chain in our trajectory analysis.

Here, it is more convenient to evaluate the extent of π-conjugation of thiophene chains by the conjugation length (CL), i.e., the number of successively coplanar π-conjugated rings (Scheme 2). The experimentally measured effective conjugation length (ECL) corresponds to the maximum value of conjugation lengths in a chain, at which the excitation energies appear size-independent.[5,37] So, the E_{ex} for a twisted thiophene chain might be mainly dependent on the ECL rather than on the whole chain length.

The percentages of the distributions of the effective conjugation length for packing systems of **3T**, **6T**, and **12T** are given in Figure 8. The most populated ECLs for **3T**, **6T**, and **12T** systems are 2, 3, and 4, respectively. The further lengthening of chains does not increase the extent of π-conjugation owing to the enhancing flexibility of a long chain, so that properties such as the maximum absorption spectra, ionization energy, and anodic peak potential of thiophene oligomers with the chain length of 5 or 6 are quite close to the corresponding data of polymer.[5] Therefore, the excitation energies of packing systems can be mainly estimated by those of the effectively conjugated fragments.

3.2 Excitation Energies of the Packing Systems. *Excitation Energies of Isolated Oligomers.* The TDDFT (B3LYP/6-311++G**) excitation energies for the first dipole-allowed excited states of planar isolated oligothiophenes as well as their experimental results[2,38,39] are listed in Table 1. In comparison with experimental results, the TDDFT excitation energy of the isolated thiophene **T** is overestimated by 0.31 eV, whereas the excitation energies of isolated longer oligothiophenes **2*n*T** ($n = 1, {}^3/_2, 2$, and 3) are underestimated by 0.28−0.54 eV. Besides the calculation error caused by the intrinsic problem of the DFT functional, ignoring the interchain interactions and chain torsions may also cause some deviations of the calculated results from the experimental values. For the isolated thiophene system, the inter-ring interaction is neglected by the TDDFT calculations. And for the real longer chain systems, **2*n*T** ($n = 1, {}^3/_2, 2$, and 3), additional deviations originate from the exaggerated planarity in the TDDFT computations on the fully conjugated model systems.

Influence of Interchain Distances. To obtain a more quantitative relationship between excitation energies and interchain distances, we perform the TDDFT/6-311++G** calculations on four models with superposed oligomer chains, **T-T**, **2T-2T**, **3T-3T**, and **4T-4T** (Figure 9) at various interchain distances.

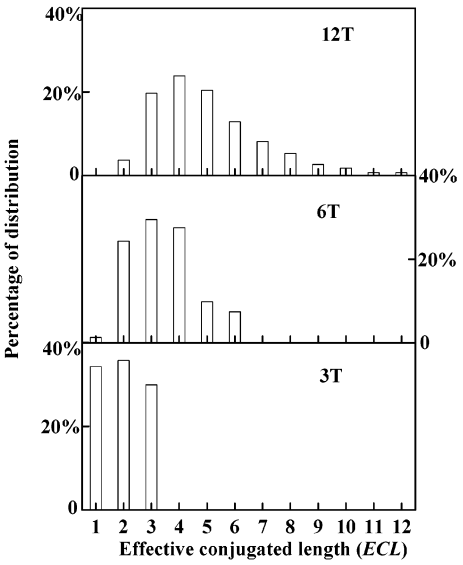

Figure 8. The statistic distribution of effective conjugation length (ECL) for terthiophene (**3T**), sexithiophene (**6T**), and duodecithiophene (**12T**) systems by MD simulations.

TABLE 1: The TDDFT/B3LYP/6-311++G Excitation Energies, E_{ex}, of the Isolated Planar Oligothiophenes, 2nT, and the Estimated Values of Packing Systems with the Experimental Results Listed for Comparison**

	E_{ex}/eV		
species	isolated oligomer	statistic estimation of system	exp/eV
$n = 1/2$	5.68	5.49	5.37[a]
$n = 1$	3.84		4.12[a]
$n = 3/2$	3.15	3.67	3.52[a]
$n = 2$	2.81		3.22[a]
$n = 3$	2.38	3.01	2.92[b]
$n = 6$		2.80	
$n = \infty$	1.69	2.47	2.2[c]

[a] Reference 38. [b] Reference 39. [c] Reference 2.

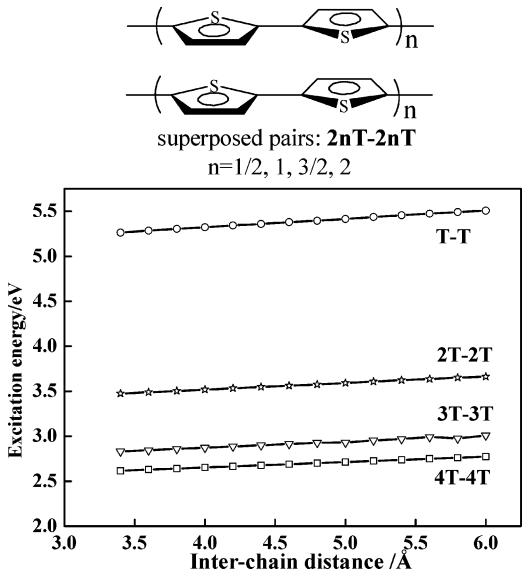

Figure 9. Effect of interchain distances on TDDFT excitation energies of the first optically allowed states of **T-T**, **2T-2T**, **3T-3T**, and **4T-4T** superposed pairs. The calculations are performed at B3LYP/6-311++G**. The oscillator strengths are in the range of 0.01−0.02.

We constrained the monolayer structure with the B3LYP/6-31+G* optimized geometry and varied the interchain distances at the internal distance of 0.5 Å. Evidently, for all the packing systems the excitation energies of the first optically allowed states, E_{ex}, decrease in a linear relationship with the narrowing interchain distances, R (Figure 9). The linear correlations can be represented in a general formula as follows:

$$E_{ex}(R) = kR + b \tag{3}$$

The fitted slopes, k, and intercepts, b, are given here: for **T-T** packing, $k = 0.093$ and $b = 4.95$; for **2T-2T** packing, $k = 0.074$ and $b = 3.22$; for **3T-3T** packing, $k = 0.066$ and $b = 2.61$; and for **4T-4T** packing, $k = 0.060$ and $b = 2.41$.

Interestingly, the values of the slopes (k) and intercepts (b) both approximately exist as a linear correlation against the reciprocal of the chain length ($1/n$), that is:

$$k = 0.02\left(\frac{1}{n}\right) + 0.05 \tag{4}$$

$$b = 1.72\left(\frac{1}{n}\right) + 1.51 \tag{5}$$

Therefore, the total relationship among excitation energies, chain lengths, and interchain distances can be roughly estimated by the following equation:

$$E_{ex}(R) = \frac{0.02R + 1.72}{n} + 0.05R + 1.51 \tag{6}$$

Since the excitation energy of a long-chain system is mainly decided by the effective conjugation length, ECL, the effects of interchain distances and chain lengths on excitation energies can be further simplified as:

$$E_{ex} = \frac{0.02R + 1.72}{\mathrm{ECL}} + 0.05R + 1.51 \qquad (R < 8.0\ \text{Å}) \tag{7}$$

When two chains are separated far beyond about 8.0 Å, their excitation energies are equal to those of their isolated chains. Therefore, the effective interchain distance to impose effects on excitation energies is taken as less than 8.0 Å, which is compatible with the analysis of the INDO/SCI wave function for the cofacial stilbene dimer that molecular orbitals are completely localized on single units when the separation is larger than 8.0 Å.[40]

The effect of the interchain distance on the excitation energy can be understood from shifts of frontier orbital levels of packing pairs relative to the isolated rings. It is well-known that the excitation energy has a close relationship to the HOMO-LUMO gap for the π-conjugated system. Here, we take the superposed thiophene dimer as an example. In a dimer, the interaction between two rings leads to a splitting of the degenerate HOMO and LUMO levels of two isolated units into four nondegenerate molecular orbitals (cf. Figure 10a). Such a splitting results in the upshifted HOMO level and downshifted LUMO level of a dimer relative to an isolated ring. Consequently, the HOMO-LUMO gap in a dimer is expected to become narrower than that of an isolated ring. From Figure 10b we can clearly see that the shorter interchain distance leads to the larger degree of the splitting and the narrower HOMO-LUMO gap in a dimer. Thereby, the excitation energies of packing pairs are gradually lowered with the decreasing interchain distances. The orbital splits also exist in systems with the more stacked units (Figure 10c). The shift in the excitation energies with the interchain distance and the number of stacked chains also may be explained by using the models developed for excimers.[41,42] In addition,

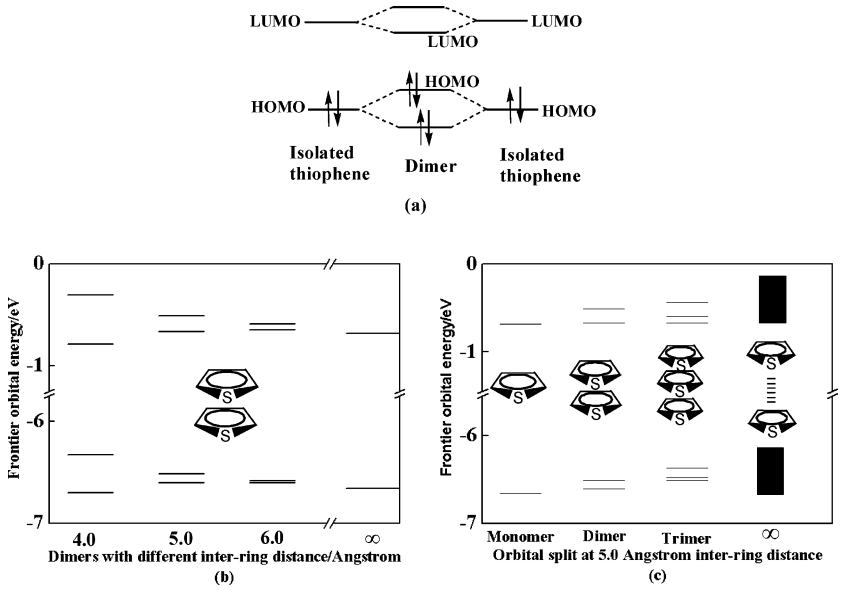

Figure 10. (a) Schematic diagram of the splitting of the degenerate HOMO and LUMO levels of the isolated units into four nondegenerate molecular orbitals and splittings with (b) different inter-ring distances of π-stacked dimers and (c) more stacked units at 5.0 Å inter-ring distance.

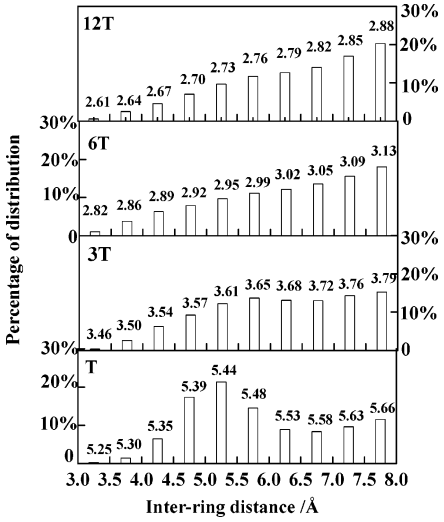

Figure 11. The statistic distribution of interchain distances at every internal of 0.5 Å. The date on the top of every column is the average value of excitation energy corresponding to each range of interchain distance.

excimer states can be easily formed with the short interchain separations and the more stacked chains, thus, the fluorescence spectrum coming from the excimer band has been observed[41] and predicted to be red-shifted with decreasing interchain distances.[42]

In addition, the slope k decreases gradually when the chain is elongated (e.g., $k = 0.074$ for **2T**-**2T** and $k = 0.060$ for **4T**-**4T** packings). The flat slope of the long-chain system indicates the effect of the interchain interaction on E_{ex} becomes weak for long packing chains, because the enhanced π-electronic delocalization along the chain backbone depresses the delocalization of π-electrons between the separated chains.

Statistic Estimations on Excitation Energies of Packing Systems. In fact, all possible packing configurations exist in a time-evolved ensemble and the experimental measurements correspond to the statistically averaged values over all possible distributions. So the excitation energy of a packing system can be estimated by a weighted average of the population of interchain distances. Since the effect of the interchain interaction on excitation energies is within the range of 8.0 Å, we only consider the statistic distribution in this range. The distributions at every interval of 0.5 Å interchain distance are plotted in Figure 11, and the averaged excitation energies corresponding to these intervals are listed on the top of the distributions. As addressed above, the effective conjugation lengths for **3T**, **6T**, and **12T** are 2, 3, and 4, respectively. Finally, the weighted averages of excitation energies for **T**, **3T**, **6T**, and **12T** systems are 5.49, 3.67, 3.01, and 2.80 eV, respectively. These values are in agreement with the experimental data (cf. Table 1) with the average deviation of 0.12 eV.

4. Conclusions

The packing structures and packing effects on excitation energies for oligothiophenes of **T**, **3T**, **6T**, and **12T** are studied by employing the MD simulations and the TDDFT calculations. Theoretical simulations show that (1) when going from the short- to long-chain systems, the packing structure prefers to be the π-stacked form and (2) the effective conjugation lengths, ECLs, of **3T**, **6T**, and **12T** are around 2, 3, and 4, respectively. The effects of the interchain distance, R, and ECL on excitation energy can be simultaneously estimated by a simple formula. The calculated excitation energies for **T**, **3T**, **6T**, and **12T** packing systems are 5.49, 3.67, 3.01, and 2.80 eV, respectively. These values are in agreement with the experimental data with the average deviation of 0.12 eV.

Acknowledgment. The authors thank two reviewers for their constructive and pertinent comments and the China NSF (No. 90303020 and No. 20103004) for the financial support.

Supporting Information Available: Figure showing the torsional potentials of bithiophene obtained from the polymer consistent force field (PCFF), consistent valence force field (CVFF), and universal force field (UFF) calculations. This material is available free of charge via the Internet at http://pubs.acs.org.

References and Notes

(1) Kertesz, M. In *Handbook of Organic Conductive Molecules and Polymers*; Nalwa, H. S., Ed.; John Wiley & Sons Ltd.: New York, 1997; Vol. 4, pp147−172.

(2) Roncali, J. *Chem. Rev.* **1997**, *97*, 173−205.

(3) (a) Brédas, J. L.; Silbey, R.; Boudreaux, D. S.; Chance, R. R. *J. Am. Chem. Soc.* **1983**, *105*, 6555−6559. (b) André, J. M.; Delhalle, J.; Brédas, J. L. W*orld Scientific Lecture and Course Notes in Chemistry*; World Scientific Publishing Co. Pte. Ltd.: Singapore, 1991; Vol. 2, and references therein.

(4) Brédas, J. L.; Street, G. B.; Thémans; André, J. M. *J. Chem. Phys.* **1985**, *83*, 1323−1329.

(5) Jones, D.; Guerra, M.; Favaretto, L.; Modelli, A.; Fabrizio, M.; Distefano, G. *J. Phys. Chem.* **1990**, *94*, 5761−5766.

(6) (a) Ortí, E.; Viruela, P. M.; Sánchez-Marín, J.; Tomás, F. *J. Phys. Chem.* **1995**, *99*, 4955−4963. (b) Distefano, G.; Dal Colle, M.; Jones, D.; Zambianchi, M.; Favaretto, L.; Modelli, A. *J. Phys. Chem.* **1993**, *97*, 3504−3509.

(7) Chadwick, J. E.; Kohler, B. E. *J. Phys. Chem.* **1994**, *98*, 3631−3637.

(8) Ehrendorfer, Ch.; Karpfen, A. *J. Phys. Chem.* **1994**, *98*, 7492−7496.

(9) De Oliveira, M. A.; Duarte, H. A.; Pernaut, J. M.; De Almeida, W. B. *J. Phys. Chem. A* **2000**, *104*, 8256−8262.

(10) Pogantsch, A.; Heimel, G.; Zojer, E. *J. Chem. Phys.* **2002**, *117*, 5921−5928.

(11) Onipko, A.; Klymenko, Y.; Malysheva, L. *J. Chem. Phys.* **1997**, *107*, 7331−7344.

(12) McCullough, R. D.; Lowe, R. D.; Jayaraman, M.; Anderson, D. L. *J. Org. Chem.* **1993**, *58*, 904−912

(13) Marseglia, E. A.; Grepioni, F.; Tedesco, E.; Braga, D. *Mol. Cryst. Liq. Cryst.* **2000**, *348*, 137−151.

(14) Brédas, J. L.; Cornil, J.; Beljonne, D.; Dos Santos, D. A.; Shuai, Z. *Acc. Chem. Res.* **1999**, *32*, 267−276.

(15) Tsuzuki, S.; Honda, K.; Azumi, R. *J. Am. Chem. Soc.* **2002**, *124*, 12200−12209.

(16) Beljonne, D.; Cornil, J.; Silbey, R.; Millié, P.; Brédas, J. L. *J. Chem. Phys.* **2000**, *112*, 4749−4758.

(17) Cornil, J.; Beljonne, D.; Dos Santos, D. A.; Calbert, J. P.; Shuai, Z.; Brédas, J. L. *Org. Electrolumin.* **2000**, *4*, 403−408.

(18) Cornil, J.; Calbert, J. Ph.; Beljonne, D.; Silbey, R.; Brédas, J. L. *Synth. Met.* **2001**, *119*, 1−6.

(19) Van Bolhuis, F.; Wynberg, H. *Synth. Met.* **1989**, *30*, 381−389.

(20) Porzio, W.; Destri, S.; Mascherpa, M.; Brückner, S. *Acta Polym.* **1993**, *44*, 266.

(21) Horowitz, G.; Bachet, B.; Yassar, A.; Lang, P.; Demanze, F.; Fave, J. L.; Garnier, F. *Chem. Mater.* **1995**, *7*, 1337.

(22) Siegrist, T.; Fleming, R. M.; Haddon, R. C.; Laudise, R. A.; Lovinger, A. J.; Katz, H. E.; Bridenbaugh, P.; Davis, D. D. *J. Mater. Res.* **1995**, *10*, 2170−2173.

(23) Siegrist, T.; Kloc, C.; Laudise, R. A.; Katz, H. E.; Haddon, R. C. *Adv. Mater.* **1998**, *10*, 379.

(24) Kertesz, M. In *Handbook of Organic Conductive Molecules and Polymers;* Nalwa, H. S., Ed.; John Wiley & Sons Ltd.: New York, 1997; Vol. 3, p 89.

(25) (a) Sun, H. *Macromolecules* **1995**, *28*, 701−712. (b) Sun, H.; Mumby, S. J.; Maple, J. R.; Hagler, A. T. *J. Phys. Chem.* **1995**, *99*, 5873−5882. (c) Hill, J. R.; Sauer, J. *J. Phys. Chem.* **1994**, *98*, 1238−1244. (d) Hwang, M. J.; Stochfisch, T. P.; Hagler, A. T. *J. Am. Chem. Soc.* **1994**, *116*, 2515−2525.

(26) Almemingen, A.; Bastiansen, O.; Svendá, P. *Acta Chem. Scand.* **1958**, *12*, 1671.

(27) Visser, G. J.; Heeris, G. J.; Wolters, J.; Vos, A. *Acta Crystallogr. B* **1968**, *24*, 467.

(28) *Cerius2*, version 3.5; Molecular Simulation Inc.: San Diego, CA, 1997.

(29) Hsu, C. P.; Hirata, S.; Head-Gordon, M. *J. Phys. Chem. A* **2001**, *105*, 451−458.

(30) Hirata, S.; Head-Gordon, M. *Chem. Phys. Lett.* **1999**, *302*, 375−382.

(31) Wiberg, K. B.; Stratmann, R. E.; Frisch, M. J. *Chem. Phys. Lett.* **1998**, *297*, 60−64.

(32) Ma, J.; Li, S.; Jiang, Y. *Macromolecules* **2002**, *35*, 1109−1115.

(33) Zhang, G.; Ma, J.; Jiang, Y. *Macromolecules*. **2003**, *36*, 2130−2140.

(34) Frisch, M. J.; Trucks, G. W.; Schlegel, H. B.; Scuseria, G. E.; Robb, M. A.; Cheeseman, J. R.; Zakrzewski, V. G.; Montgomery, J. A., Jr.; Stratmann, R. E.; Burant, J. C.; Dapprich, S.; Millam, J. M.; Daniels, A. D.; Kudin, K. N.; Strain, M. C.; Farkas, O.; Tomasi, J.; Barone, V.; Cossi, M.; Cammi, R.; Mennucci, B.; Pomelli, C.; Adamo, C.; Clifford, S.; Ochterski, J.; Petersson, G. A.; Ayala, P. Y.; Cui, Q.; Morokuma, K.; Malick, D. K.; Rabuck, A. D.; Raghavachari, K.; Foresman, J. B.; Cioslowski, J.; Ortiz, J. V.; Baboul, A. G.; Stefanov, B. B.; Liu, G.; Liashenko, A.; Piskorz, P.; Komaromi, I.; Gomperts, R.; Martin, R. L.; Fox, D. J.; Keith, T.; Al-Laham, M. A.; Peng, C. Y.; Nanayakkara, A.; Challacombe, M.; Gill, P. M. W.; Johnson, B.; Chen, W.; Wong, M. W.; Andres, J. L.; Gonzalez, C.; Head-Gordon, M.; Replogle, E. S.; Pople, J. A. *Gaussian 98*, Revision A.9; Gaussian, Inc.: Pittsburgh, PA, 1998.

(35) Bucci, P.; Longerini, M.; Veracini, C. A.; Lunazzi, L. B. *J. Am. Chem. Soc.* **1974**, *96*, 1305.

(36) Alberti, A.; Favaretto, L.; Seconi, G.; Pedulli, G. F. *J. Chem. Soc., Perkin Trans. 2* **1990**, 213.

(37) Martin, R. E.; Gubler, U.; Boudon, C.; Bosshard, C.; Gisselbrecht, J. P.; Günter, P.; Gross, M.; Diederich, F. *Chem. Eur. J.* **2000**, *6*, 4400−4412.

(38) Diaz, A. F.; Crowley, J.; Bargon, J.; Gardini, G. P.; Torrance, J. B. J. *Electroanal. Chem.* **1981**, *121*, 355−361.

(39) Van Haare, J. A. E. H.; Havinga, E. E.; Van Dongen, J. L. J.; Janssen, R. A. J.; Cornil, J.; Brédas, J. L. *Chem. Eur. J.* **1998**, *4*, 1509−1522.

(40) Cornil, J.; Dos Santos, D. A.; Crispin, X.; Silbey, R.; Brédas, J. L. *J. Am. Chem. Soc.* **1998**, *120*, 1289−1299.

(41) Xu, B.; Holdcroft, S. *Macromolecules*. **1993**, *26*, 4457−4460.

(42) Piryatinski, A.; Deck, R. T. *Chem. Phys. Lett.* **1997**, *269*, 156−160 and references therein.